J Solid State Electrochem (2011) 15:2619–2631
DOI 10.1007/s10008-010-1241-3

ORIGINAL PAPER

FTIR spectroscopic characterization of Nafion®–polyaniline composite films employed for the corrosion control of stainless steel

Despina Kosseoglou · Rebecca Kokkinofta · Dimitra Sazou

Received: 28 August 2010 / Revised: 7 November 2010 / Accepted: 9 November 2010 / Published online: 1 December 2010
© Springer-Verlag 2010

Abstract Nafion®–polyaniline (PAn) composite films deposited by a two-step process on a stainless steel (SS) substrate were characterized in this study using Fourier transform infrared (FTIR) spectroscopy under various conditions employed to evaluate their anticorrosion pro perties. The SS|Nafion® electrode was first prepared by placing a certain amount of Nafion® on the SS substrate, and then polymerization of aniline was carried out potentiodynamically on the SS|Nafion® electrode. The SS|Nafion®–PAn electrodes subjected to both potentiodynamic polarization and open-circuit conditions in sulfuric acid solutions without and with chlorides appeared to have distinct differences in their FTIR spectra. It is proposed that under the electrochemical conditions used in this study, the PAn is mostly formed inside the Nafion® membrane with a high proportion of oligomers influencing the ionic transport through the membrane. The inhibition of pitting corrosion arises primarily from the enhanced permselectivity of the composite film due to the Nafion® membrane that prevents chloride transport. An essential beneficial effect comes also from the PAn redox properties on the growth of the passive oxide film. Even under severe corrosion conditions, Nafion®–PAn films retain their redox activity and chemical stability, whereas the membrane crystallinity seems to be enhanced.

D. Kosseoglou · D. Sazou (✉)
Department of Chemistry, Aristotle University of Thessaloniki,
54124, Thessaloniki, Greece
e-mail: sazou@chem.auth.gr

R. Kokkinofta
State General Laboratory,
44 Kimonos Str.,
1451, Nicosia, Cyprus

Keywords Composite Nafion®–PAn membranes · Stainless steel · Corrosion control · FTIR spectroscopic characterization

Introduction

The preparation of hybrid materials has attracted remarkable scientific and technological interest in recent years. Composite with Nafion® intrinsic electronic conducting polymers in which electronic and ionic properties are combined provide materials with enhanced mechanical properties and improved dynamics of the doping–undoping process [1–5]. Previously, Nafion®-doped polyaniline (PAn) thin films deposited on AISI 304 stainless steel (SS) were studied in terms of their protective properties against pitting corrosion of the alloy substrate [6, 7]. Among other applications [8], PAn is used as the basis for the formation of anticorrosive coatings deposited either electrochemically or chemically on oxidizable metals and alloys [6–10]. These composite coatings attracted great interest in recent years as environmentally friendly materials for corrosion control. Towards the improvement of the mechanical stability and protective efficiency of PAn coatings, several approaches were followed such as blending of PAn with conventional polymers [9], co-polymerization [7, 10], and doping with large anions such as ionomers [6, 7]. Unlike PAn doped with small anions, which readily exchange with solution anions (i.e., Cl^-), the doping by ionomers leads to a stable composite material where only proton exchange occurs during redox processes [4]. Other strategies were also followed to improve the protective efficiency of conducting polymers used as anticorrosive coatings.

Nafion® is a chemically inert, cation perm-selective material with high ionic conductivity [11, 12]. Because of

these properties, Nafion® membranes have been used in many electrochemical applications, earlier in chloro-alkali industry in electrodialysis [13] and in recent years in proton-exchange membrane fuel cells due to their good proton conductivity [14]. Although Nafion® is characterized by good chemical and mechanical stability, progress is still needed in order to enhance its performance depending on the targeted application (i.e., in chloro-alkali cells, rechargeable batteries [15], ion-selective electrodes [16] etc.). Modification of the Nafion® membrane is often carried out by using a variety of fillers, i.e., SiO_2 [17, 18], inorganic acids [19, 20], or polymers, i.e., poly(1-vinylimidazole) [21]. Another method used for the modification of the Nafion® membrane is the "filling" with conducting polymers such as PAn [1–10, 22–27], PAn along with SiO_2 [28], poly(*o*-anisidine) [29] or polypyrrole [30–35]. Nafion®–PAn composites have been mostly explored because they comprise the electronic conductivity of PAn with the ionic conductivity of Nafion®. PAn inclusions were found to affect the diameter of transport channels in composite membranes and hence the efficiency of electromembrane separation processes [24–26].

Protection by PAn-based coatings has often been ascribed to the enhancement of the formation of passive oxide film on the metal substrate resulting in the shift of the interface equilibrium potential to more positive values [36–39]. As was shown previously, the protective properties of PAn against pitting corrosion of SS in chloride-containing sulfuric acid solutions are enhanced by using the Nafion® membrane as a polymerization matrix due to the cation-selective properties of the membrane that prevent the chloride transport through it [6]. Composite Nafion®–PAn films were deposited on SS surfaces by a two-step process. The Nafion® membrane cast on the SS was followed by the electrochemical polymerization of the aniline (An) by using the cyclic potential sweep (CPS) deposition technique. Increasing potential cycling results in the increase of anodic and cathodic currents indicating the growth of PAn. At the end of the CPS deposition (20 potential cycles) of An, a compact dark-green Nafion®–PAn composite film was obtained in contrast to the powdery dark-green PAn film formed on SS. The obtained Nafion®–PAn films exhibit an increasing redox current during successive potential cycling in corrosive environments where they appear to be more stable for longer periods of time compared with simple PAn films. Enhanced protective properties of the Nafion®–PAn composite films were also found by monitoring the open-circuit potential (E_{OC}) of the SS|Nafion®–PAn and SS|PAn electrodes in the same corrosive environments.

The aim of this work is the use of the Fourier transform infrared (FTIR) spectroscopy for the characterization of the modified Nafion® membranes after the polymerization of An within the Nafion® matrix as well as after a series of treatments carried out to test the protective performance of the Nafion®–PAn films in corrosive media. The issues to be addressed using the FTIR spectroscopy are first discussed demonstrating the main features of the composite and simple PAn films deposited on the SS passive surface. The coated electrodes are either subjected to potentiodynamic polarization or immersed in solutions under open-circuit conditions. The FTIR spectra of the modified Nafion®–PAn composite films were compared with those of simple Nafion® and PAn films in order to understand how the molecular structure of the composite film influences its protective properties in corrosion control studies of the SS surfaces.

Experimental

The voltammetric measurements were performed by using a VoltaLab 40 electrochemical system accompanied with the VoltaMaster 4 software from Radiometer Analytical. The working electrode was the cross section of a stainless steel (SS; AISI 304) wire 3 mm diameter (surface area= 0.0709 cm^2) embedded in a 1-cm-diameter PTFE cylinder. SS AISI 304 was purchased from Goodfellow Metals (Cambridge). A volume of 100 mL was maintained in a three-electrode electrochemical cell. A Pt sheet of a large surface area (2.5 cm^2) and a saturated calomel electrode in a KCl solution were used as counter and reference electrodes, respectively.

PAn films were deposited electrochemically (by sweeping the potential between −0.2 and 1.1 V with a sweep rate equal to dE/dt=20 mVs^{-1}) from aqueous 0.5 M H_2SO_4 solution containing 0.1 M An prepared with H_2SO_4 (Merck, pro-analysis 96% *w*/*w*) and freshly distilled aniline (Fluka, puriss p.a.) using twice-distilled water. A rotating SS-disc electrode at ω=250 rpm was used for the growth of PAn on bare SS. Nafion® films were prepared by placing 89.6 μL of Nafion® 117 (equivalent weight 1,100) 5*w*/*v*% dissolved in a mixed solution of low aliphatic alcohols and water onto the SS by using a micropipette. The SS electrode was placed under a glass cover to shield the electrode from irregular air stream until a film was formed. The Nafion® films were dried for 24 h at room temperature before use. The stock Nafion 117 solution was purchased from Aldrich (Hydrogen Ion Form, Cat. No 27,470-4). The solution for electrochemical polymerization was de-aerated with purified N_2 for 20–25 min before the beginning of each experiment. Measurements were carried out at room temperature, 22±2°C. Before each experiment, the SS-disc electrode was polished by a series of wet sandings using different grit sizes (100, 180, 320, 500, 800, 1,000, 1,200, and superfine). After mechanical polishing, SS was rinsed first with twice-distilled water and after with ethanol under ultrasonic agitation for 30 s in each solution.

To access the protective properties of both the composite Nafion®–PAn and PAn films, open-circuit potential measurements were carried out along with potentiodynamic current–potential (*I*–*E*) curves traced at $dE/dt=10\ mV\,s^{-1}$ in chloride-containing solutions such as 0.5 M H_2SO_4+0.5 M NaCl in comparison with chloride-free 0.5 M H_2SO_4. NaCl was purchased from Fluka and was puriss p.a. in purity. The maximum quantity of PAn in simple and composite with Nafion® films can be estimated by using the amount of charge involved in the first (~29 mC for the PAn film) and tenth potential cycles (~1.58 mC for the Nafion®–PAn film), respectively, obtained from the cyclic volammograms ($dE/dt=10\ mV\,s^{-1}$) traced from the An-free 0.5 M H_2SO_4 (Fig. 1c, d). On the basis of Faraday's first law, it is found that the simple PAn films contain $\sim 2.1\times10^{-3}$ mmol cm^{-2}, whereas the Nafion®–PAn films contain $\sim 1.2\times10^{-4}$ mmol cm^{-2}.

The procedure to prepare the samples before FTIR spectroscopic characterization is as follows: samples were washed thoroughly with twice-distilled water after their removal for the test solutions and dried at room temperatures for 7 days. These samples were in partially drying state because they contained residual water [35, 40, 41]. FTIR spectra were recorded on a Schimatzu 9000 FTIR spectrometer with a wavenumber resolution of 2 cm^{-1} in the range of 400–4,000 cm^{-1}. Membrane samples were mixed with KBr powders and pressed to pellets. The spectra were obtained against the air background spectrum. Scanning electron microscopic micrographs were taken with a JEOL JSM-840A Scanning Electron Microscope (SEM).

Results and discussion

Electrochemical properties of the composite Nafion®–PAn films and their protective capability in comparison with the behavior of simple PAn films

The composite films used in this study were formed on the SS|Nafion® electrode by employing CPS deposition as was described in detail previously [7] and mentioned briefly in previous sections. Figure 1a illustrates selected cyclic voltammograms of the SS|Nafion® electrode in 0.5 M H_2SO_4 containing 0.1 M An traced during the first ten potential cycles at a sweep rate $dE/dt=20\ mV\,s^{-1}$. The polymerization of An at a Nafion®-free SS electrode is also shown in Fig. 1b for the sake of comparison. Comparing the progress of the two polymerization processes (Fig. 1a, b), it is obvious that (1) the polymerization rate is higher on bare SS than on the Nafion®-coated SS electrode as redox current indicates, and (2) there exist a stronger shift of the anodic/cathodic peak potential to more/lesser positive values during the An polymerization within the Nafion® matrix than on Nafion®-free SS due to the lower conductivity of the SS|Nafion® electrode compared with that of the passive SS.

Scanning electron microscopy (SEM) images shown in the insets of Fig. 1 compare the morphology of PAn grown on the two electrodes. The Nafion®–PAn film (inset of Fig. 1a) seems to be compact, and it does not display any particular morphology, which it might be in nano-size dimensions. This image indicates a good homogenization

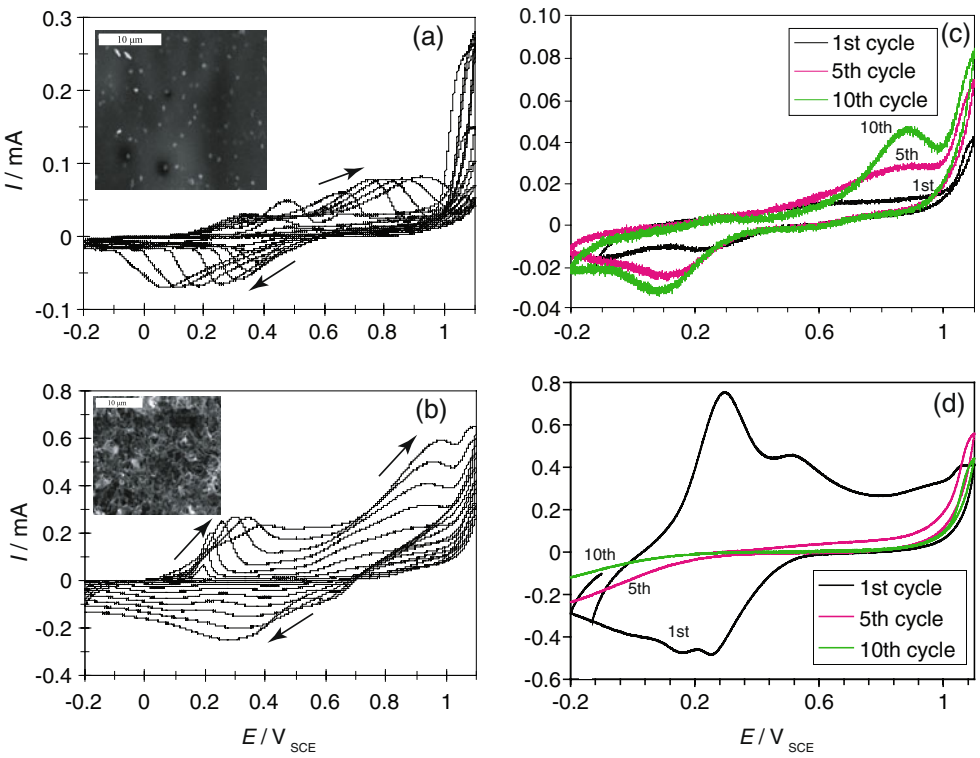

Fig. 1 Successive cyclic voltammograms for the first ten cycles recorded at $dE/dt=20\ mV\,s^{-1}$ during the growth of PAn on: **a** SS|Nafion® and **b** SS in 0.5 M H_2SO_4 containing 0.1 An. *Insets* illustrate SEM micrographs revealing the morphology of the prepared films. The electrochemical response of the **c** SS|Nafion®–PAn and **d** SS|PAn electrodes (prepared using 20 potential cycles) in An-free 0.5 M H_2SO_4 traced at $dE/dt=10\ mV\,s^{-1}$

of PAn within the Nafion® matrix, resulting in a smooth layer. Light spots observed over the surface indicate perhaps that a certain amount of PAn is formed outside of the Nafion® matrix [3, 6]. On the other hand, the PAn film (inset of Fig. 1b) seems to be porous displaying aggregates of particles with dimensions ranged between 100 and 200 nm. Differences in the morphology of the two films may arise from the fact that degradation reactions occur to a higher degree during the polymerization on SS than within the Nafion® membrane. In fact, comparing the electrochemical response during consecutive cycles of the composite Nafion®–PAn (Fig. 1c) and simple PAn film (Fig. 1d) traced in An-free 0.5 M H_2SO_4 solution indicates clearly that degradation is prevented to a high degree in the case of the composite film.

The electrochemical response of the PAn and composite Nafion®–PAn films was traced after removing the SS|Nafion®–PAn and SS|PAn electrodes from the polymerization solution and rinsing them thoroughly with distilled water to ensure that monomer is removed completely from the electrode surface. Two redox peaks appear during the first cycle for both composite Nafion®–PAn (Fig. 1c) and simple PAn films (Fig. 1d), which are attributed to the oxidation of the reduced PAn (leucoemeraldine) to the partly oxidized PAn (emeraldine, EM) around 0.2–0.3 V and to a further oxidation of the EM to the fully oxidized PAn (pernigraniline) at more positive potentials. Redox currents of the composite film increase during consecutive cycles of the potential between −0.2 and 1.1 V (Fig. 1c). The increase of the current continues up to several cycles, depending on the Nafion® membrane thickness and PAn amount [42], which under these particular conditions is found to be approximately ten cycles. This increase of the current is not fully understood, and FTIR characterization is anticipated to throw light to this behavior. On the contrary, the current of the SS|PAn electrode traced under the same conditions with those of Fig. 1c decreases during successive potential cycling, whereas the peak potentials of the redox process shifts essentially (Fig. 1d). It is suggested that this behavior arises from degradation processes when sweeping towards potentials higher than 0.8 V. Degradation results in soluble products such as benzoquinone and/or *p*-aminophenol, which would reduce the amount of the deposited polymer [43, 44].

The improved protective ability of the Nafion®–PAn composite films compared with that of simple PAn ones is mostly assigned to the prevention of chloride insertion into the cation-selective composite film. The insertion of Cl^- that reaches the substrate surface is expected to result in pitting corrosion, which manifests itself by high dissolution currents. To test the insertion of Cl^- into the films, the electrochemical response of the SS|Nafion®–PAn and SS|PAn electrodes was further examined in acid and neutral chloride-containing solutions. Figure 2 shows that during the potentiodynamic polarization at $dE/dt = 10\ mV\,s^{-1}$ in the 0.5 M H_2SO_4+0.5 M NaCl solution the SS|Nafion®–PAn electrode retains its redox activity (Fig. 2a) during successive cycling, while the SS|PAn electrode does not (Fig. 2b), leading to relatively high dissolution currents. It should be noticed that PAn provides a partial protection only during the first potential cycle where a kind of redox behavior can be seen by using an appropriate scale (Fig. 2c). However, the protective efficiency of PAn diminishes essentially during successive potential cycling due to the insertion of Cl^-. The shape of the cyclic voltammograms shown in Fig. 2b indicates that chlorides result in pitting corrosion of SS despite the presence of the PAn film. This is also confirmed by visual as well as SEM observations. An example of the substrate with open pits after the potentiodynamic response of the SS|PAn electrode in chloride-containing solutions is shown in Fig. 2e. On the contrary, the SS|Nafion®–PAn electrode seems to be resistible to pitting corrosion under the same potentiodynamic conditions, and open pits on the SS substrate are not detected in SEM images (Fig. 2d). Table 1 summarizes comparatively an estimation of the pitting corrosion potential E_{pit} and the maximum current I_{max} obtained at the first sweep during reverse potential cycling of the studied coated and non-coated SS electrodes.

Additionally, the E_{OC} was monitored in 0.5 M H_2SO_4 for 2 h and then in 0.5 M H_2SO_4+0.5 M NaCl for also 2 h [7]. Table 1 shows that the E_{OC} of both the SS|Nafion®–PAn and SS| PAn electrodes shifts to higher values compared with that of either the bare SS or SS| Nafion® electrodes and attains values that correspond to the passive state of SS. The E_{OC} remains constant for a very long time in the chloride-free solution. The E_{OC} of all electrodes remains at values close to those obtained after 2 h as Fig. 3a shows. A significant shift of the E_{OC} to lower values associated with fluctuations appears in the presence of Cl^- for the PAn-coated electrodes (Fig. 3b). Fluctuations of the E_{OC} are attributed to early stages of pitting corrosion involving local activation–passivation events that are reflected to the decrease–increase of the E_{OC}, respectively [39]. Figure 3b shows that the E_{OC} of the SS|Nafion®–PAn electrode shifts only slightly during the first 2 h but remains in the passive state within a considerably longer time without fluctuations [6, 7]. One should notice that, although the solution where electrodes were tested is a very aggressive one, the Nafion®–PAn membrane provides such a protection against pitting corrosion that neither the passive oxide film of SS nor the PAn film does.

A drawback of the composite films exposed to corrosive media, which appeared only in certain cases after the removal of the samples from the solution, is the poor mechanical stability of films. Few films exhibited crack defects especially

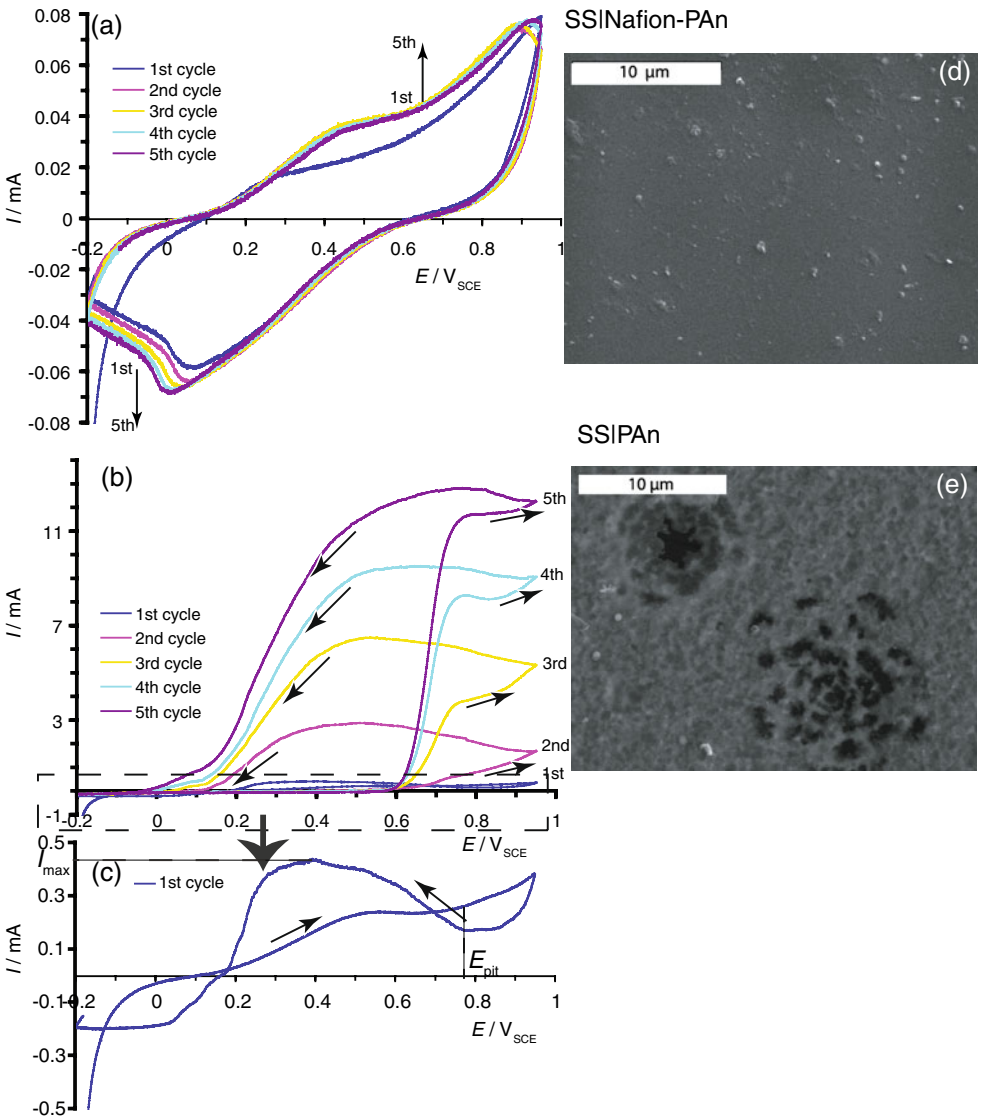

Fig. 2 Electrochemical response of the: **a** SS|Nafion®–PAn and **b**, **c** SS|PAn electrodes in 0.5 M H_2SO_4+0.5 M NaCl at dE/dt=10 mVs^{-1}; **d**, **e** SEM micrographs of the SS substrate after cyclic potentiodynamic polarization (first cycle between −0.2 and 1.1 V and second cycle between −0.5 and 1.6 V) of the SS|PAn and SS|Nafion®–PAn electrodes in 0.5 M H_2SO_4+ 0.5 M NaCl

after immersion in chloride-containing solutions. This is due perhaps to changes in the water or ion content of the membrane that may lead to structural changes of the ionomer backbone [24–27]. Another reason might be related to the adhesion of the membrane to the oxide-coated SS substrate. The higher the degree of adhesion, the more positive the E_{OC} should be expected due to the prevention of solution transport that may result in corrosion of the SS substrate within a shorter time. Indeed, more systematic studies showed that the E_{OC} of the SS|Nafion®–PAn electrode is related to the value of the E_{OC} of the SS|Nafion® electrode measured before the polymerization process [42].

Table 1 Pitting potential (E_{pit}) and maximum dissolution current (I_{max}) values obtained during potentiodynamic polarization of the electrodes in 0.5 M H_2SO_4+0.5 M NaCl along with open-circuit potential (E_{OC}) values of the various electrodes observed after 2 h of immersion in 0.5 M H_2SO_4 and 2 h in 0.5 M H_2SO_4 + 0.5 M NaCl

Electrode	0.5 M H_2SO_4	0.5 M NaCl+0.5 M H_2SO_4		
	E_{OC} (V)	E_{OC} (V)	E_{pit} (V)	I_{max} (mA)
SS|Nafion®–PAn	0.48	0.40	No pitting	PAn redox current
SS|Pan	0.50	0.15	~0.78	~0.43 (first cycle)
SS|Nafion®	0.18	0.10	~0.55	~0.043 (first cycle)
SS	−0.43	−0.46	~0.55	~63

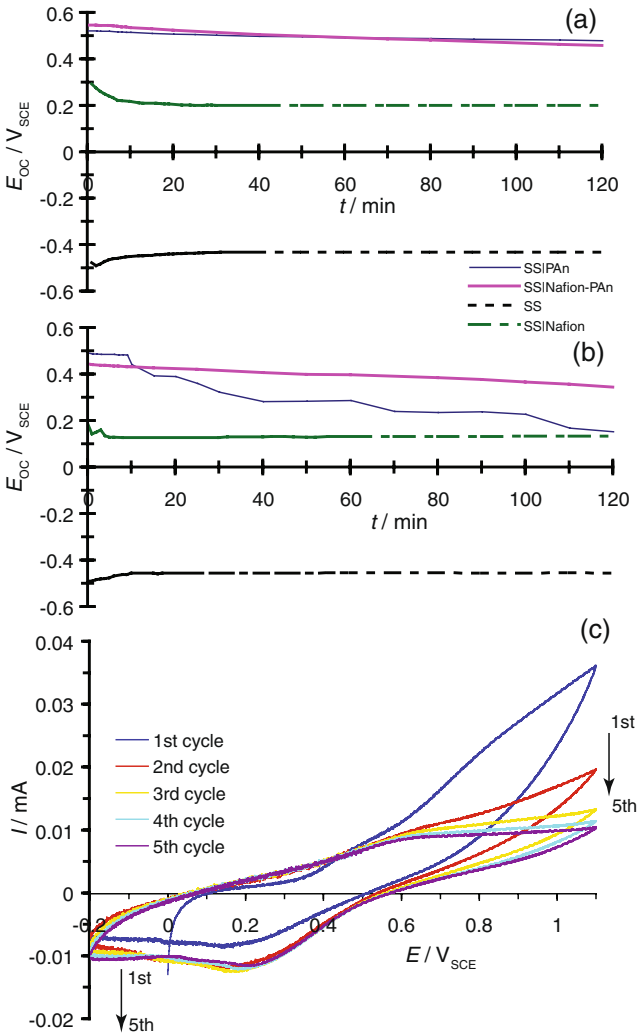

Fig. 3 Comparative plots of the open-circuit potential, E_{OC}, vs. time for the various electrodes in **a** 0.5 M H_2SO_4 and **b** 0.5 M H_2SO_4+ 0.5 M NaCl; **c** electrochemical response of the SS|Nafion®–PAn electrode in 0.5 M NaCl at dE/dt=10 mVs^{-1} during successive potential cycling between −0.2 and 1.1 V

In principle, the improved protection performance of the Nafion®–PAn film against pitting corrosion of SS in chloride-containing solutions should be understood by considering that the PAn within the Nafion® membrane is in its fully protonated form. Presumably, sulfonate groups of the membrane can act as dopants and thus keep the protons within the composite film, whereas the involvement of chlorides seems unlikely due to the permselectivity of the Nafion® membrane. Indeed, it was shown that the Nafion® membranes implanted with PAn chains exhibit enhanced permselectivity attributed to the fact that PAn chains remain mainly in their positively charged state [22, 45]. This property of composite films is expected to be useful in corrosion control studies by extending the application of Nafion®–PAn films in neutral and even basic media where PAn loses to a great extent its redox activity. An example of this behavior is illustrated in Fig. 3c, which shows the first five potential cycles of the SS|Nafion®–PAn electrodes in neutral 0.5 M NaCl solutions by cycling in the region between −0.2 and 1.1 V at dE/dt=10 mVs^{-1}. The electroactivity of PAn seems to be very good, and redox currents increase during potential cycling although to a lesser degree than in acidic solutions (Fig. 1c). Pitting corrosion is not detected even after 20 potential cycles.

In summary, from the brief survey of the electrochemical behavior of Nafion®–PAn films in conjunction with their anticorrosion properties, the FTIR spectroscopic characterization under various test conditions is anticipated to throw light to molecular/structural changes of the composite membrane related to the following: (1) the redox states of PAn within the membrane, (2) the increase of the electroactivity of the Nafion®–PAn films during consecutive potential cycling on the contrary to simple PAn films, (3) doping effect of Nafion® sulfonate groups, and (4) chemical and mechanical stability of composite membranes. All films for which FTIR spectroscopic measurements were taken after various test conditions are summarized in Table 2.

FTIR spectroscopic characterization of PAn and Nafion®

The FTIR spectrum of PAn is shown in Fig. 4a. The characteristic bands with their assignation are summarized in Table 3. These infrared bands are in agreement with those given in the literature [46–53]. The baseline over the region 4,000–2,000 cm^{-1} is raised notably, indicating that PAn is in its doping form. The N–H stretching region appears over ~3,600–3,000 cm^{-1} with a peak centered at 3,440 cm^{-1} assigned to the symmetrical stretching vibration of NH_2 while the asymmetrical one appears as an ill-defined shoulder at ~3,560 cm^{-1}. The C–H stretching within the absorption region 3,000–2,800 cm^{-1} is weak, indicating saturated benzene rings [52], whereas the sharp peak at 1,640 cm^{-1} represents N–H deformation. The absorption of PAn in regions 1,600–1,580 and 1,500–1,480 cm^{-1} corresponds to stretching vibrations of quinoid (Q) and benzenoid (B) rings indicating that PAn and oligomers are composed of imine and amine units [53]. In particular, the stronger peak at 1,473 cm^{-1} is assigned to the N–B–N stretching of the B ring, whereas the weaker peak at 1,570 cm^{-1} is characteristic of the Q ring. Other peaks near B and Q bands are also associated to the corresponding stretching in aniline oligomers [50]. The low intensity of B and Q bands is attributed to the high doping level of the polymer. It was observed that by increasing the degree of doping, the intensity of B and Q bands decreases and becomes red-shifted [49]. Particularly, in the case of the

Table 2 Modified SS electrodes used for the FTIR spectroscopic characterization

Number of electrode	Film	Preceding treatment
0	PAn	Equilibration at ambient conditions
1	Nafion®	Equilibration at ambient conditions
2	Nafion®–PAn	Immediately after polymerization[a]
3	Nafion®–PAn-10	CVs over 10 potential cycles in 0.5 M H_2SO_4[a]
4	Nafion®–PAn-Cl	CV over 1 potential cycle in 0.5 M H_2SO_4+0.5 M NaCl[a]
5	Nafion®–PAn-OCP	Monitoring OCP for 1 h in 0.5 M H_2SO_4[a]
6	Nafion®–PAn-OCP-Cl	Monitoring OCP for 1 h in 0.5 M H_2SO_4 and next for 1 h in 0.5 M H_2SO_4+0.5 M NaCl[a]

Simple PAn and composite Nafion®–PAn films were prepared by CPS deposition over 20 potential cycles in the region between −0.2 and 1.1 V in 0.5 M H_2SO_4+0.1 M An

[a] Equilibration at ambient conditions was followed for each test

PAn formed from the H_2SO_4 solution, the latter bands are red-shifted compared, for instance, with the corresponding bands of the PAn formed from HCl because both Q and B bands are more protonated [49].

In the C–N stretching region for aromatic amine, there is one band of low intensity at 1,380 cm^{-1} and two peaks of equal intensity at ~1,307 and 1,245 cm^{-1}. According to Tang et al. [48], the band at 1,380 cm^{-1} is assigned to C–N stretching in QB_tQ structure, whereas the peak at 1,307 cm^{-1} represents QB_cQ, QBB, and BBQ structures, and the peak at 1,245 cm^{-1} is assigned to BBB structure (Table 3). The relatively broad band at 1,138 cm^{-1} represents the vibration mode of the $–NH^+=$ structure formed after protonation. The band at 1,138 cm^{-1} is referred as a measure of the extent of delocalization of electrons on PAn and is characteristic of the PAn conductivity [49, 53]. In the range of in-plane and out of plane bending of C–H bonds on aromatic ring, there are peaks at 1,022 and 995 cm^{-1} as well as absorption peaks at 887 and 840 cm^{-1}. Bands at 1,022 and 995 cm^{-1} along with peaks at 1,138 and 1,303 cm^{-1} indicate 1,4-substitution on the benzene ring, whereas peaks at 887 and 840 cm^{-1} along with small peaks within the region 800–700 cm^{-1} support the occurrence of 1,2- and 1,3- substitution. This is due to the relatively high potential used for the CPS deposition of PAn.

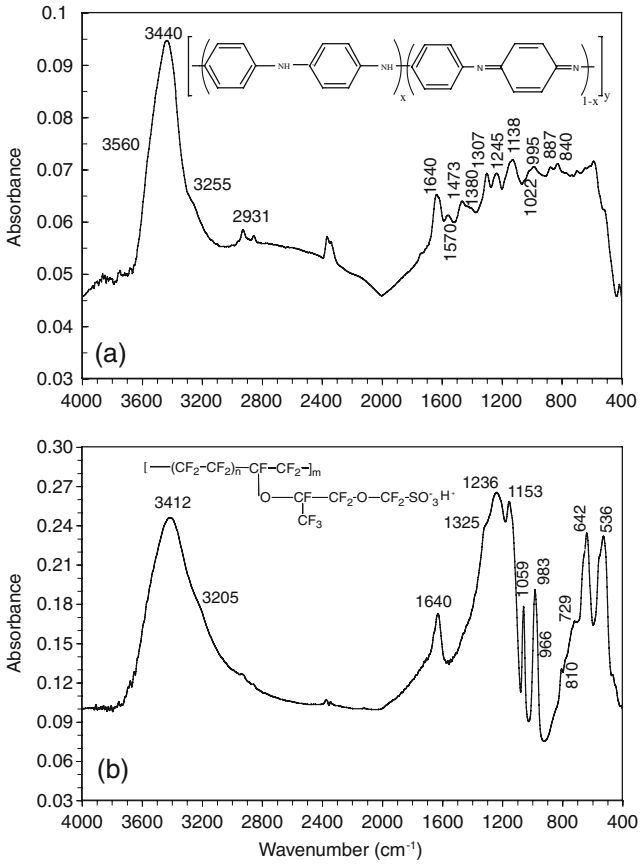

Fig. 4 FTIR spectra in the spectral region between 4,000 and 400 cm^{-1} of **a** PAn synthesized by CPS deposition between −0.2 and 1.1 V over 20 potential cycles in 0.5 M H_2SO_4 containing 0.1 M An and **b** Nafion® membrane in its protonated form

Figure 4b shows the FTIR spectrum of the protonated Nafion® membrane (H-Nafion®). Characteristic infrared bands and their assignation for the PAn-free Nafion® are presented in Table 4. The band at 3,412 cm^{-1} is assigned to the O–H stretching of water and that at 1,640 cm^{-1} along with the shoulder at 3,205 cm^{-1} to the hydrated H_3O^+ [11, 12, 40, 41, 54–61]. The peak intensity at 3,412 cm^{-1} was used by Rieke and Vanderborgh [56] to determine the water in Nafion®, and that of the band at 1,640 cm^{-1} was used by Levy et al. [57] as a quantitative indication of water in poly-perfluorosulfonic acid membrane. The absorption bands at 1,325, 1,236, and 1,153 cm^{-1} are assigned to the CF_2 backbone [11, 56, 59]. The absorption peak observed at 1,059 cm^{-1} is assigned to the symmetric vibration of the dissociated sulfonic group. The anti-symmetric stretching bands of the $–SO_3H$ group at 1,410 and 910 cm^{-1} assigned as S=O and S–OH stretching bands [40], respectively, do not appear clearly. The S=O band is masked by the strong

Table 3 FTIR characteristic bands of PAn synthesized by CPS deposition over 20 potential cycles within the potential region −0.2 and 1.1 V

Frequency (cm^{-1})	Assignment
3,600–3,000	N–H stretching region of NH_2
2,931	H-bonding, NH, NH^+
1,640	N–H deformation
1,570	Quinonoid (N=Q=N) stretching vibrations
1,473	Benzenoid (N–B–N) stretching vibrations
1,380	C–N stretching in QB_tQ environment
1,307	C–N stretching in QB_cQ, QBB, BBQ environment (π-electron delocalization)
1,245	C–N^+ stretching in the benzenoid structure (BBB) (polaron formation)
1,138	Q=NH^+-B formed during protonation
1,022, 995	C–H in-plane bending in aromatic rings (1,4 substitution)
887, 840, 800–700	C–H out-of-plane bending in aromatic rings (1,2 or 1,3 substitution)

t and c in QB_tQ and QB_cQ stand for trans- and cis-, respectively, whereas Q and B stand for quinonoid and benzenoid rings, respectively

C–F stretching vibration band at ~1,300 cm^{-1} [41]. Vibrational bands associated with the $–SO_3H$ and $–SO_3^-$ groups are useful in providing information about the H^+ transport and the coordination behavior [41]. The absorption peak appeared at 983 cm^{-1} with a shoulder at ~966 cm^{-1} are assigned as stretching modes with mixed C–O–C and CF character [41, 57]. The change of the position of these peaks depends on the chemical environment adjacent to the membrane. The region between 800 and 500 cm^{-1} represents mostly C–F groups [56, 59–61]. However, stretching of C–S, δS–O, and M–O (hydrates and oxides of metal from the SS substrate) within the latter band region could not be ruled out [35].

FTIR spectroscopic characterization of the composite Nafion®–PAn films

The FTIR spectra of the Nafion®–PAn films are shown in Fig. 5 (whole spectral region, 4,000–400 cm^{-1}) and Fig. 6 (region 1,700–400 cm^{-1}) for different measurement conditions (Table 2). All films were dried and equilibrated under same ambient conditions. As can be seen in Fig. 5, noticeable differences are observed in the absorbance around 3,412 cm^{-1} and the spectral region between 2,000 and 400 cm^{-1}. Comparing with the FTIR spectrum of the simple Nafion®, one notices that the Nafion® bands around 3,412 and 1,640 cm^{-1} diminish in intensity for all PAn-modified Nafion® films, indicating that composite films are less hydrophilic than bare Nafion® in agreement with previous observations [23]. The water content in the measured composite films (Table 2) follows the order

Table 4 FTIR characteristic bands of Nafion® membrane in its protonated form

Frequency (cm^{-1})	Assignment
3,412	H_2O
1,640	Hydrated H_3O^+
1,325	CF_2 backbone
1,236	CF_2 asymmetric stretching
1,153	CF_2 symmetric stretching
1,059	SO_3^- symmetric stretching
983, 966 (sh)	C–O–C symmetric stretching
729 (sh)	C–S stretching
642, 663 (sh)	CF_2 wag
536, 560 (sh)	CF_2 wag or scissor

sh shoulder

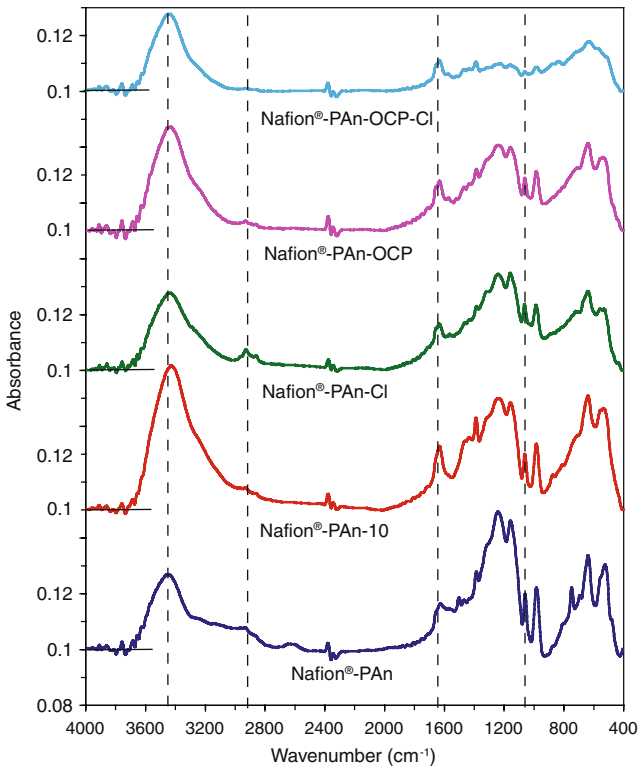

Fig. 5 FTIR spectra of the composite Nafion®–PAn films summarized in Table 2 in the spectral region between 4,000 and 400 cm^{-1}

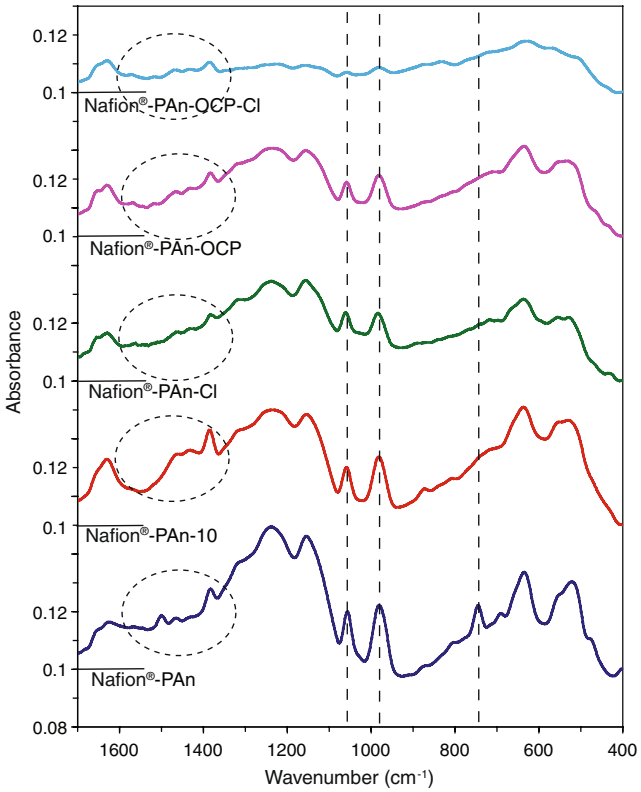

Fig. 6 Enlargement of the spectral region between 2,000 and 400 cm^{-1} for the FTIR spectra shown in Fig. 5

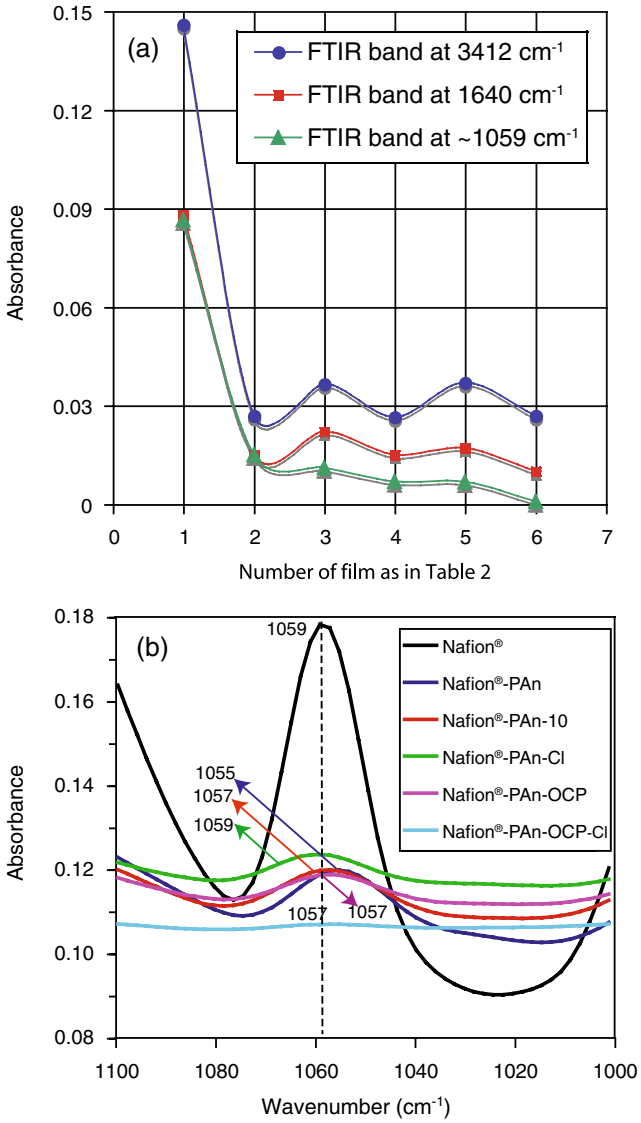

Fig. 7 **a** FTIR spectral peak absorbance at about 3,410, 1,640, and 1,059 cm^{-1} and **b** FTIR absorption spectra of the $-SO_3^-$ symmetric stretching region of the bare Nafion® and composite Nafion®–PAn films treated under the conditions shown in Table 2

shown in Fig. 7a. It seems that either after successive potential cycling or immersion in 0.5 M H_2SO_4 the intensity of these peaks increases, indicating that the water uptake in composite films increases to a higher degree under the same conditions than after other treatments of the Nafion®–PAn membrane. Partial ionization of sulfonic groups is expected as long as any water is present in the membrane [62–64].

Indeed, at a first glance, similar variation with that of the intensity at 3,412 and 1,640 cm^{-1} is also observed for the absorbance of the symmetric $-SO_3^-$ stretching peak at about 1,059 cm^{-1} (Fig. 7a). As will be discussed below, there exist slight differences attributed to both the different hydration level and the position of PAn chains within the membrane. Similarities, however, suggest that under all conditions the water is mostly in the form of the H_3O^+ ion [35]. There is a transfer of the proton resulting in the dissociated sulfonate group. The hydrated Nafion® membrane contains both labile H^+ associated with the water and electrostatically bound H^+ that originate from the SO_3^- group [63]. Bound H^+ contributes to the protonation of the PAn in the oligomer or polymer form that counterbalance the negative charge of the SO_3^- groups. The degree of hydration and the type of counterion both affect also significantly the position of the bands of sulfonate groups [63]. Figure 7b shows a shift of the position of $-SO_3^-$ stretching band depending on the ionic environment or chemical surroundings of the sulfonate group. The shift of the band at 1,059 cm^{-1} is due to the polarization of the S–O dipole by the electrostatic field of adjacent counterions [23, 61].

The presence of PAn in the composite with Nafion® films is manifested by the absorbance at ~1,570 (Q band), ~1,475 (B band), and ~1,380 (QB_tQ) cm^{-1} (t stands for trans). Close to Q and B bands, there appear additional bands attributed to the quinoid and benzenoid stretching modes of An oligomers [50]. Figure 6 shows that more benzenoid groups exist in the as-formed Nafion®–PAn and Nafion®–PAn-10 composite films than in the simple

PAn (Fig. 4a), suggesting that PAn is mostly in the emeraldine salt state in the composite film. The multiple peaks near the Q and B bands seem to be eliminated in the Nafion®–PAn-10, indicating the incorporation of oligomers into the main polymer chain during consecutive cyclic voltammetry. The bands at 1,245 and 1,138 cm^{-1} assigned, respectively, to C–N stretching in BBB and C–H bonds in aromatic rings of the PAn are less noticeable in the composite films because they are superimposed on the broad CF_2 band. This leads to a broader band within the 1,300–1,100 cm^{-1} spectral region for the composite films than the one corresponding to the bare Nafion® (Fig. 4b).

The results presented in previous sections indicate that FTIR spectroscopy may lead to a further understanding of issues (1)–(4) raised in the first subsection. These issues, discussed in the following subsections, are mainly related with the molecular/structural changes of the composite Nafion®–PAn membranes when they are used in severe corrosion environments.

Redox states and protonation level of the PAn within the nanocomposite Nafion® membrane

The different redox states of the PAn chain associated with its doping level and protonation extent within the Nafion® matrix and Nafion® surface will be first discussed in order to get an insight regarding issues (1) and (2). The bands observed at the range ~1,570–1,560 (Q) and 1,498–1,430 (B) are very sensitive to the oligomer chain structure. Q and B bands appear to be doublet in the as-formed composite film that may be assigned to the presence of An oligomers. On the contrary to simple PAn films, dissolution and in turn removal of oligomers is not facilitated in the Nafion® matrix during electropolymerization via CPS deposition. This fact is consistent with the increase in the current observed for the SS|Nafion®–PAn electrodes during successive potential cyclic in An-free sulfuric acid solutions (Fig. 1c) and is reflected in FTIR spectra. As can be seen in Fig. 6, doublet Q and B bands tend to become single when the Nafion®–PAn is subjected to ten potential cycles. Moreover, the intensity of the B band is more than double the intensity of the Q band, indicating incorporation into the polymer chain of either oligomers or even anilium molecules that exist at the membrane surface [64]. A more uniform Nafion®–PAn film is obtained, which had an emerald-green color.

The relatively high density of the C–N stretching in QB_tQ at ~1,380 cm^{-1} ensures that PAn is in the emeraldine salt state in agreement with the improved protective ability of the Nafion®–PAn-10 film in Cl^--containing solutions [6]. In view of these facts and the mechanism by which PAn acts as an active protective coating against metallic corrosion [6, 39], it should be suggested that successive potential cycling of the Nafion®–PAn in An-free sulfuric acid solutions strengthens the PAn chain through a further incorporation of either oligomers or anilinium existing at different positions of the hydrophilic side of the ionomer. Besides the increase of the current during potential cycling, this fact results in a positive shift of the oxidation peak potential due rather to changes of the ionic transport in composite membranes. It is suggested that PAn is formed either in the hydrophilic clusters of the Nafion® where anilinium forms ion pairs first with sulfonate groups or in the intermediate region located between the hydrophobic and the hydrophilic regions blocking the transport of cations within the membrane [23]. A more positive redox potential of the composite film is expected to maintain the passive state of the SS in corrosive media manifested by the more positive E_{OC} observed in acid media without and with the presence of chlorides (Table 1).

The red-shifted C–N stretching bands in the neighborhood of the QBQ and BBB structures of the Nafion®-doped PAn after polarization in either H_2SO_4 or Cl^--containing H_2SO_4 (Table 5) indicates that PAn becomes more protonated than the as-formed composite films. This explains the higher conductivity of the films appearing

Table 5 Shifts of vibrations upon treatment of composite Nafion®–PAn films (no. 2–6) under different conditions as shown in Table 2 with respect to bare Nafion® (no. 1)

	1	2	3	4	5	6
Free H_2O	3,412	3,450	3,425	3,429	3,425	3,434–3,435
H_3O^+ ?	1,628	1,622	1,628	1,628	1,628	1,628
CF_2 asymm. str.	1,236	1,236	1,234	1,236	1,234	1,220
CF_2 symm. str.	1,153	1,153	1,151	1,155	1,157	1,155
ν_s (S–O)	1,059	1,055	1,057	1,059	1,057	1,057
ν (C–O–C)	982	980	980	982	980	980
ν (C–S) + others	636	633	635	635	635	629
δ (C–O)	525–529	519–523	528	528	532	509 (vw)
C–N in QB_tQ	–	1,385	1,387	1,390	1,388	1,389
N–B–N	–	1,464	1,462	1,458	1,464	1,466
N=Q=N	–	1,566	1,514	1,533	1,568	1,570

during consecutive cycling (Fig. 1c) leading to a better stability of the composite film even in the presence of Cl^- (Figs. 2a and 3c). Moreover, this behavior is in agreement with previous observations showing that the PAn backbone can be modified by the nearby species, which affect primarily the Q and B segments [44]. Thus, the increase in the conductivity is not solely due to the water uptake manifested by the increase in the intensity in the spectral region 3,800–1,500 cm^{-1}.

Changes in the spectra are observed during monitoring the E_{OC} with time in sulfuric acid solutions without and with chlorides at wavenumbers below 2,000 cm^{-1} in the range of C–N stretching indicating deprotonation under open-circuit conditions. For instance, a blue shift of the band at 1,566 cm^{-1} occurs in latter solutions (Table 5). Indeed, an enhanced deprotonation is expected to occur in acidic solutions in the presence of NaCl where protons may be exchanged with Na^+. This deprotonation process explains also the lower currents observed during successive cycling in neutral solutions of NaCl (Fig. 3c), which appear in almost half of those traced in NaCl-containing acidic solutions (Fig. 2a). This is in agreement with experimental data suggesting that Nafion® in its protonic form has a higher conductivity and lower diffusion permeability [65].

Doping effect of the Nafion® sulfonate groups

Water molecules and sulfonate groups play the most important role in the function of the composite H-Nafion® membranes [11]. The nanostructure of the composite Nafion®–PAn films is expected to result from both the SO_3H–PAn and SO_3H–H_2O interactions along with the geometry of the hydrophobic backbone. Therefore, the ionic interactions between the SO_3^- group and the positively charged groups of PAn (issue (3)) will be discussed.

A shift of the band at 1,059 cm^{-1} attributed to the S–O symmetric stretching indicates a change in polarization of the S–O dipole by the ionic environment [23, 35, 61, 66]. It was observed that the SO_3^- band shifts to lower values in the presence of either monovalent or divalent cations or certain polymeric chains. It is suggested that the larger the amount of positively charged groups are interacting with the SO_3^- groups, the greater the shift of the SO_3^- band to lower values. However, in the presence of PAn in the Nafion®, Tan and Belanger [23] have observed a very little shift (~2 cm^{-1}). Furthermore, Park et al. [35] have also observed a similar little shift in the presence of polypyrrole in Nafion®. A red shift of a similar extent was also observed in the present study (Fig. 4b). It seems that stronger interactions are developed after potential cycling in sulfuric acid solutions (Nafion®–PAn-10) in agreement with the higher conductivity that as was discussed above it stems from a higher degree of protonation. In fact, sulfonate groups of the Nafion® membrane act as dopants and keep the protons within the PAn.

Since the shift of the symmetric stretching vibration of the SO_3^- group provides also valuable information about the effect of the environment on the exchange properties of the membrane, it may be deduced from Table 5 that under various corrosive conditions the exchange properties of the composite membranes do not alter drastically. Additionally, it should be noticed that the behavior of the SO_3^- functional groups within the ionomer matrix depends also on the H_2O. Sulfonate groups and water molecules play an important role in the formation of the proton conductivity network in composite Nafion®–PAn membrane. The 3,800–1,500 cm^{-1} region depends on the H_2O and H_3O^+ content. Thus, comparison of this FTIR region in the modified Nafion® membranes with that of the bare H-Nafion® leads to a rough evaluation of the water content. Comparing with the literature, the water content in the unmodified H-Nafion is ~16% (~10 water molecules) and in the composite Nafion®–PAn is evaluated as ~3 %. This water content remains either constant as it was observed under conditions that involved NaCl in the solutions or becomes higher (4–6%) under other conditions. This shows that composite films retain their permselectivity in agreement with the good protective properties shown even in severe corrosive environments (Figs. 2 and 3 and Table 1).

Therefore, in terms of FTIR spectral data and in agreement with electrochemical data, the electrochemically synthesized PAn within the Nafion® membrane ($RSO_3^-H_3O^+$) seems to involve the following steps:

1. A cation exchange process: protons are exchanged with anilinium (An^+) cations, $RSO_3^-H_3O^+ + An^+ \leftrightarrows RSO_3^-An^+ + H_3O^+$.
2. Oxidation of anilinium, $RSO_3An \rightarrow RSO_3An^{+\cdot} + e$.
3. Formation of aniline oligomer and polymer chains inducing ionomer structural changes.
4. Interchain redox reactions involved membrane protons.

Chemical and mechanical stability of the nanocomposite Nafion®–PAn membranes

A last issue to be discussed is related to changes in the chemical stability and structure of the composite films that should certainly affect their protection performance. The FTIR spectra of all Nafion®–PAn films including those exposed for 2 h in 0.5 M H_2SO_4 and then for 2 h in 0.5 M H_2SO_4+0.5 M NaCl show the characteristic peaks of Nafion® at 1,236, 1,153 (CF_2), and 980 cm^{-1} (mixed C–O–C and CF_2). Table 5 shows that the position of these

peaks is influenced only slightly by changes in PAn chains within the membrane, possibly due to the no-polarity of this membrane segment. Thus, the modified composite membranes retain the basic chemical structure. This is in agreement with the behavior shown in Fig. 3 where it is illustrated that even after seven cycles in neutral 0.5 M NaCl the main redox peaks hardly changed indicating the chemical stability of composite films. It should be noticed that Cl^- was not found in energy dispersive X-ray analysis of the composite films. The negatively charged sulfonate groups present within the Nafion® prevent the transport of negatively charged Cl^- through the composite films by Donnan exclusion. However, chloride transport remains to be examined within a longer-term exposure of the composite films to chloride-containing solutions. Under severe corrosive environments, some metal ions from SS may be released and should influence the permeability of the Nafion®–PAn membrane as well as the ionic transport through the membrane.

FTIR spectral changes appear mostly in the region between 800 and 500 cm^{-1}, which might be associated with variations of the Nafion® crystallinity [41]. The main changes are: (1) an almost elimination of a band between 700 and 800 cm^{-1}, (2) increase in the ratio of bands at 641 and 628 cm^{-1}. These changes along with no broadening of the band at 511 cm^{-1} are consistent with an enhanced crystallinity of the composite membranes after various treatments as compared with the as-formed Nafion®–PAn membrane. Variations of the membrane crystallinity might be related with the decrease of the mechanical stability of the composite membrane that appeared in some cases after a long-term exposure in the corrosive solutions.

Conclusions

FTIR spectroscopy was used to characterize composite Nafion®–PAn films deposited first electrochemically on SS and then subjected to different severe corrosion conditions. The main goal of this study was to get a better understanding of the molecular/structural changes of the Nafion®–PAn nanocomposite membrane when it is used to inhibit localized corrosion of the SS substrate. From the results presented, it is deduced that by varying the electrochemical conditions during preparation of the composite films, it is possible to obtain Nafion®–PAn composite films with a different length and oxidation states of the polymer chain either on the surface or the inner phase of the Nafion® membrane. Particularly the increase of conductivity during successive cycling results in a uniform composite film of an emerald-green color with improved protective properties due to the insertion of the anilinium into the polymeric chain towards the bulk of the membrane and an increase of protonation. It is shown that a relatively long-term immersion of the Nafion®–PAn films in a sodium chloride sulfuric acid solution under open-circuit conditions causes significant structural changes associated with deprotonation due to transport of metal cations from both sites of the film, Na^+ from the solution site and perhaps M^{x+} cations (perhaps M≡Fe, Cr) from the SS|oxide site. However, as the FTIR spectra show, the chemical stability of composite films remains fairly good, whereas their crystallinity seems to be enhanced under all conditions.

Acknowledgments We thank Dr. Evroulla Hapeshi and Christothea Attipa for their assistance in obtaining the FTIR spectra.

References

1. Barthet C, Guglielmi M (1995) J Electroanal Chem 388:35–44
2. Barthet C, Guglielmi M (1996) Electrochim Acta 41:2791–2798
3. Alpatova NM, Andreev VN, Danilov AI, Molodkina EB, Polukarov Yu M, Berezina NP, Timofeev SV, Bodrova LP, Belova NN (2002) Russ J Electrochem 38:913–918
4. Orata D, Buttry DA (1987) J Am Chem Soc 109:3574–3581
5. Orata D, Buttry DA (1988) J Electroanal Chem 257:71–82
6. Sazou D, Kosseoglou D (2006) Electrochim Acta 51:2503–2511
7. Sazou D, Kourouzidou M (2009) Electrochim Acta 54:2425–2433
8. Inzelt G (2008) In: Scholz F (ed) Conducting polymers: a new era in electrochemistry. Springer, Berlin
9. de Souza S (2007) Surf Coat Technol 201:7574–7581
10. Pawar P, Sainkar SR, Patil PP (2007) J Appl Polym Sci 103:1868–1878
11. Heitner-Wirguin C (1996) J Membrane Sci 120:1–33
12. Mauritz KA, Moore RB (2004) Chem Rev 104:4535–4585
13. Yeo RS, Yeager HL (1985) in: Conway BE, White RE, Bockris JO'M (eds) Modern Aspects of Electrochemistry, vol. 16: 437–504
14. Grot W (2008) Fluorinated ionomers. William Andrew Publishng, NY
15. Li N, Lee JY, Ong LH (1992) J Appl Electrochem 22:512–516
16. Do J-S, Chang W-B (2004) Sensors & Actuators B 101:97–106
17. Baradie B, Dodelet JP, Guay D (2000) J Electroanal Chem 489:101–105
18. Miyake N, Wainright JS, Savinell RF (2001) J Electrochem Soc 148:A905–A909
19. Malhotra S, Datta R (1997) J Electrochem Soc 144:L23–L26
20. Dimitrova P, Friedrich KA, Stimming U, Vogt B (2002) Solid State Ionics 150:115–122
21. Bae BC, Ha HY, Kim D (2005) J Electrochem Soc 152:A1366–1372
22. Tan S, Viau V, Cugnod D, Bélanger D (2002) Electrochem Sol St Letters 5:E55–E58
23. Tan S, Bélanger D (2005) J Phys Chem B 109:23480–23490
24. Compañ V, Riande E, Fernandez-Carretero FJ, Berezina NP, Sytcheva AA-R (2008) J Membrane Sci 318:255–263
25. Berezina NP, Kononenko NA, Sytcheva AA-R, Loza NV, Shkirskaya SA, Hegman N, Pungor A (2009) Electrochim Acta 54:2342–2352
26. Berezina NP, Kubaisy AA, Timofeev SV, Karpenko LV (2007) J Solid State Electrochem 11:378–389
27. Berezina NP, Kononenko NA, Loza NV, Sytcheva AA-R (2007) Rus J Electrochem 43:1340–1349
28. Chen C-Y, Garnica-Rodriquez JI, Duke MC, Dalla Costa RF, Dicks AL, da Costa JC Diniz (2007) J Power Sources 166:324–330

29. Bertoncello P, Notargiacomo A, Riley DJ, Ram MK, Nicolini C (2003) Electrochem Commun 5:787–792
30. Yoneyama H, Hirai T, Kuwabata S, Ikeda O (1986) Chem Lett 1243–1246.
31. Fan F-RF, Bard AJ (1986) J Electrochem Soc 133:301–304
32. Easton EB, Langsdorf BL, Hughes JA, Sultan J, Qi Z, Kaufman A, Pickup PG (2003) J Electrochem Soc 150:C735–C739
33. Langsdorf BL, MacLean BJ, Halfyard JE, Hughes, Pickup PG (2003) J Phys Chem B 107:2480–2484
34. Langsdorf BL, Sultan J, Pickup PG (2003) J Phys Chem B 107:8412–8415
35. Park H, Kim YJ, Hong WH, Choi YS, Lee HK (2005) Macromolecules 38:2289–2295
36. Spinks GM, Dominis AJ, Wallace GG, Tallman DE (2002) J Solid State Electrochem 6:73–84
37. Spinks GM, Dominis AJ, Wallace GG, Tallman DE (2002) J Solid State Electrochem 6:85–100
38. Zarras P, Anderson N, Webber C, Irvin DJ, Irvin JA (2003) Radiat Phys Chem 68:387–394
39. Sazou D, Kourouzidou M, Pavlidou E (2007) Electrochim Acta 52:4385–4397
40. Ludvigsson M, Lindgren J, Tegenfeldt J (2000) Electrochim Acta 45:2267–2271
41. Gruger A, Régis A, Schmatko T, Colomban Ph (2001) Vibrat Spectroscopy 26:215–225
42. Kosseoglou D, Sazou D (2006) 57th Annual Meeting of the ISE in Edinburg.
43. Stilwell DE, Park S-M (1988) J Electrochem Soc 135:2254–2262
44. Stilwell DE, Park S-M (1988) J Electrochem Soc 135:2491–2496
45. Sata T, Ishii Y, Kawamura K, Matsusaki K (1999) J Electrochem Soc 146:585–591
46. Salaneck WR, Liedberg B, Inganas O, Erlandsson R, Lundstrom I, MacDiarmid AG, Halpen M, Somasiri NLD (1985) Mol Cryst Liq Cryst 121:191–194
47. Cao Y, Li S, Xue Z, Guo D (1986) Synth. Met 16:305–315
48. Tang J, Jing X, Wang B, Wang F (1988) Synth Met 24:231–238
49. Trchová M, Sedenková I, Tobolkova E, Stejskal J (2004) Polym Degrad Stability 86:179–185
50. Coates J (1997), in: Meyers RA (Ed), Encyclopedia of Analytical Chemistry, John Wiley & Sons, pp 1–23.
51. Kang ET, Neoh KG, Tan KL (1998) Prog Polym Sci 23:277–324
52. Prasad KR, Munichandraiah N (2001) Synth Met 123:459–468
53. Chiang J-C, MacDiarmid AG (1986) Synth Met 13:193–205
54. Moynihan RE (1959) J Am Chem Soc 81:1045–1050
55. Heitner-Wirguin C (1979) Polymer 20:371–374
56. Rieke PC, Vanderborgh NE (1987) J Membrane Sci 32:313–328
57. Levy LY, Jenard A, Hurwitz HD (1982) J Chem Soc Faraday Trans I 78:17–29
58. Buzzoni R, Bordiga S, Ricchiardi G, Spoto G, Zecchina A (1995) J Phys Chem 99:11937–11951
59. Perusich SA (2000) Macromolecules 33:3431–3440
60. Falk M (1980) Can J Chem 58:1495–1501
61. Lowry SR, Mauritz KA (1980) J Am Chem Soc 102:4665–4667
62. Zawodzinski TA Jr, Derouin C, Radzinski S, Sherman RJ, Smith VT, Springer TE, Gottesfeld S (1993) J Electrochem Soc 140:1041–1047
63. Seger B, Vinodgopal K, Kamat PV (2007) Langmuir 23:5471–5476
64. Tan S, Tieu JH, Belanger D (2005) J Phys Chem B 109:14085–14092
65. Berezina NP, Kubaisi AA-R (2006) Rus J Electrochem 42:81–88
66. Tannenbaum R, Rajagopalan N, Eisenberg A (2003) J Polym Sci B: Polym Phys 41:1814–1823